HHS Public Access

Author manuscript

Hum Genet. Author manuscript; available in PMC 2019 July 01.

Published in final edited form as:

Hum Genet. 2018 July ; 137(6-7): 459–470. doi:10.1007/s00439-018-1898-8.

De Novo variants in *GREB1L* are associated with non-syndromic inner ear malformations and deafness

Isabelle Schrauwen[1,2,*], **Elina Kari**[3], **Jacob Mattox**[4], **Lorida Llaci**[2], **Joanna Smeeton**[5], **Marcus Naymik**[2], **David W. Raible**[6], **James A. Knowles**[7], **J. Gage Crump**[5], **Matthew J. Huentelman**[2,¶], and **Rick A. Friedman**[3,¶]

[1]Center for Statistical Genetics, Molecular and Human Genetics Department, Baylor College of Medicine, One Baylor Plaza, Houston, TX 77030

[2]Neurogenomics Division and Center for Rare Childhood Disorders, Translational Genomics Research Institute, 445 N 5th str, Phoenix, AZ 85004

[3]Division of Otolaryngology, Head and Neck Surgery, Department of Surgery, University of California, San Diego, ECOB- East Campus Office Building Room 3-013, 9444 Medical Center Drive, Mail Code 7220, La Jolla, CA 92037

[4]Tina and Rick Caruso Department of Otolaryngology- Head and Neck Surgery, Keck University of Southern California School of Medicine, 1975 Zonal Ave., Los Angeles, CA 90033

[5]Department of Stem Cell Biology and Regenerative Medicine, University of Southern California Keck School of Medicine, 1975 Zonal Ave., Los Angeles, CA 90033

[*]Corresponding Author: Isabelle Schrauwen, Center for Statistical Genetics, Molecular and Human Genetics Department, Baylor College of Medicine, One Baylor Plaza, Houston, TX, isabelle.schrauwen@gmail.com. Tel: +1 713 7986844.

[¶]These authors contributed equally to this work.

Supplementary Material

Supplemental Data can be found with the online version of this manuscript and includes a Supplementary Figures document with eight figures (Figs S1-S8) and 3 tables (Tables S1–3). Genetic variations have been deposited in ClinVar (Accession numbers #SCV000611707 and #SCV000611708).

Compliance with Ethical Standards

Institutional review board (IRB) approval for human research was obtained, and the principles outlined in the Declaration of Helsinki were followed. Informed consent was obtained from the participants involved (University of Southern California (USC) IRB #HS-14-00513-CR002 and Western (IRB) #20120512). The Institutional Animal Care and Use Committee of the USC approved the animal experiments performed in this study (No. 10885). The authors declare that they have no conflict of interest.

Web Resources

Bravo TOPMed variant browser, https://bravo.sph.umich.edu/
Burrows-Wheeler Aligner, http://bio-bwa.sourceforge.net/
CDC, hearing loss in children, http://cdc.gov/ncbddd/hearingloss/data.html/
Clinvar, https://www.ncbi.nlm.nih.gov/clinvar/
Combined Annotation Dependent Depletion (CADD), http://cadd.gs.washington.edu/
dbNSFP, https://sites.google.com/site/jpopgen/dbNSFP/
dbSNP, https://www.ncbi.nlm.nih.gov/projects/SNP/
Database of Genomic Variants (DGV), http://dgv.tcag.ca/dgv/app/home/
DatabasE of genomiC varIation and Phenotype in Humans using Ensembl Resources (DECIPHER), https://decipher.sanger.ac.uk/
Exome Aggregation Consortium (ExAC), http://exac.broadinstitute.org/
Genome Aggregation Database (gnomAD), http://gnomad.broadinstitute.org/
Genome Analysis Toolkit (GATK), https://software.broadinstitute.org/gatk/
Genome Browser, https://genome.ucsc.edu/
Online Mendelian Inheritance of Man (OMIM), https://www.omim.org/
Picard, http://broadinstitute.github.io/picard/

[6]Department of Biological Structure, University of Washington, 1959 NE Pacific Street, Seattle, WA 98195

[7]SUNY Downstate Medical Center, Department of Cell Biology - MSC 5, 450 Clarkson Avenue, BSB 2-5, Brooklyn, NY 11203

Abstract

Congenital inner ear malformations affecting both the osseous and membranous labyrinth can have a devastating impact on hearing and language development. With the exception of an enlarged vestibular aqueduct, non-syndromic inner ear malformations are rare, and their underlying molecular biology has thus far remained understudied.

To identify molecular factors that might be important in the developing inner ear, we adopted a family-based trio exome sequencing approach in young unrelated subjects with severe inner ear malformations. We identified two previously unreported *de novo* loss-of-function variants in *GREB1L* [c.4368G>T;p.(Glu1410fs) and c.982C>T;p.(Arg328*)] in two affected subjects with absent cochleae and 8th cranial nerve malformations. The cochlear aplasia in these affected subjects suggests that a developmental arrest or problem at a very early stage of inner ear development exists, e.g. during the otic pit formation. Craniofacial Greb1l RNA expression peaks in mice during this time-frame (E8.5). It also peaks in the developing inner ear during E13–E16, after which it decreases in adulthood.

The crucial function of Greb1l in craniofacial development is also evidenced in knockout mice, which develop severe craniofacial abnormalities. In addition, we show that *Greb1l*$^{-/-}$ zebrafish exhibit a loss of abnormal sensory epithelia innervation. An important role for Greb1l in sensory epithelia innervation development is supported by the 8th cranial nerve deficiencies seen in both affected subjects.

In conclusion, we demonstrate that GREB1L is a key player in early inner ear and 8th cranial nerve development. Abnormalities in cochleovestibular anatomy can provide challenges for cochlear implantation. Combining a molecular diagnosis with imaging techniques might aid the development of individually tailored therapeutic interventions in the future.

Keywords

GREB1L; hearing loss; deafness; congenital inner ear malformation; 8th cranial nerve; developing inner ear

Introduction

Functional loss of hearing is one of the most common losses of sensory function with a considerable impact on quality of life and daily functioning. Nearly 2–3 per 1,000 newborns suffer from some degree of hearing loss ranging from mild to profound in the United States each year. The heterogeneous nature of hearing loss and the necessity to fine-tune multiple synchronized processes within the inner ear is supported by the large number of genes that have been linked to hereditary hearing loss so far. Up to approximately 3% of children with a profound sensorineural hearing loss (SNHL) may have cochlear and/or cochlear nerve

aplasia or hypoplasia; although, as imaging techniques improve the number of children identified is likely to increase (Kaplan et al. 2015).

Congenital SNHL in children can be due to membranous or membranous and osseous anomalies. Most children with congenital SNHL show a normal inner ear morphology on CT and MRI imaging (i.e. a normal bony labyrinth) (Sennaroglu and Bajin 2017). Their hearing loss is assumed to be the result of dysfunctions of the membranous inner ear. The genetics of this latter group is studied very well, with over 100 genes identified for non-syndromic hearing loss alone; however, all genes involved in syndromic and non-syndromic SNHL have not yet been identified.

A variety of inner ear malformations of both the membranous and bony labyrinth have been previously described amongst patients with SNHL (Pryor 2005; Masuda et al. 2013). A very common inner ear malformation seen in children with non-syndromic hearing loss is enlarged vestibular aqueduct syndrome (EVAS) (Pryor 2005). EVAS can be uni- or bilateral, and is associated with either non-syndromic or syndromic forms of SNHL, such as Pendred syndrome (PS). The majority of cases of PS and non-syndromic EVAS are due to variants in *SLC26A4* (Pryor 2005), which encodes for an anion transporter pendrin. Other cases of EVAS are found in syndromes such as branchio-oculo-facial syndrome, CHARGE syndrome, or Waardenburg syndrome (Pryor 2005). Another gene causing non-syndromic inner ear malformations is the *POU3F4* gene, causing X-linked deafness (DFNX2) (Yamamoto et al. 2017). Other than the mentioned above, there are a variety of other syndromes which include inner ear malformations, such as syndromic Michel's aplasia (*FGF3*), Down syndrome (Trisomy 21), Trisomy 13, Trisomy 18, DiGeorge syndrome (22q11.2 deletion), and Duane-radial ray syndrome (Yamamoto et al. 2017). A classification system for malformations of the osseous and membranous inner ear, which is based the various stages of embryogenesis of the inner ear, has been widely adopted (Jackler et al. 1987; Sennaroglu and Saatci 2002) (Figs S1 and S2).

In addition to the osseous and/or membranous malformations, the cochleovestibular nerve (CVN), also called the 8th cranial nerve, can be affected as well. This nerve connects the inner ear to the brainstem and enables the transmission of hearing and balance information. Abnormal CVNs (i.e., as absent, aplastic, or deficient) are rare congenital malformations that have a devastating impact on hearing and language development. They are frequently associated with inner ear abnormalities but may be found in patients without abnormalities. Abnormal CVNs are commonly associated with developmental delay syndromes, particularly CHARGE syndrome, Rapadilino syndrome, Mobius, and Duane-radial ray syndrome (Birman et al. 2016; Yamamoto et al. 2017); however, they can occur in otherwise healthy children. We recently identified compound heterozygous *MASP1* variants in a child with non-syndromic hearing loss and absent cochlear nerves (Kari et al. 2017). There is no clear consensus on the classification of CVN malformations. Birman *et al.* suggested a grading from grade 0 (no nerve in the internal auditory canal) to grade V (normal nerves) (Birman et al. 2016). This grading system is based on MRI findings of nerves within the internal auditory canal (IAC) and the size of the cochlear nerve (CN). A normal nerve anatomy shows 4 nerves in the IAC: the facial, two branches of the vestibular nerve, and the CVN.

With the exception of EVAS, non-syndromic cases of inner ear malformations of both the membranous and bony labyrinth are rare, and not well studied in genetics. This is also the case for non-syndromic abnormal CVNs. In this study, we used a trio-based exome sequencing approach to identify a new genetic defect in two young affected subjects with non-syndromic abnormal CVNs and/or inner ear malformations, affecting their hearing and speech.

Material and Methods

Clinical evaluation

Institutional review board (IRB) approval for human research was obtained from the local IRB committees, and written informed consent was obtained from all participating family members. Magnetic resonance imaging (MRI) was used to characterize inner ear abnormalities. Hearing was evaluated through auditory brainstem response (ABR) and behavioral testing. Additional tests were done to exclude other possible abnormalities, including: cranial nerve examinations, brain magnetic resonance imaging (MRI), a physical exam, and urinalysis. A renal ultrasound was performed in affected subject 1.

Exome Sequencing

DNA samples from the affected subjects and parents were collected with the iSWAB DNA buccal collection kit (Mawi DNA Technologies, Hayward, CA), and DNA was extracted with the DNeasy Blood & Tissue kit (Qiagen, Hilden, Germany). Next, exomic libraries were prepared with the TruSeq Exome Library Prep Kit using 12-plex sample pooling (Illumina Inc, San Diego, USA), following the manufacturer's protocol. Sequencing was performed by 100bp paired-end sequencing on a HiSeq2500 instrument (Illumina Inc, San Diego, USA), targeting a mean on-target coverage of 50x. Filtered reads were aligned to the Human genome (Hg19/GRC37) using the Burrows-Wheeler transform method (BWA-MEM) (Langmead et al. 2009). Reads were sorted, and PCR duplicates were removed using Picard. Base quality recalibration and indel realignments were performed using the Genome Analysis Toolkit (GATK) (McKenna et al. 2010). SNP and Indel variants were called jointly with HaplotypeCaller and recalibrated with GATK, annotated with dbNSFP and snpEff for protein-coding events (Cingolani et al. 2012; Liu et al. 2016). Prediction scores were loaded from dbNSFP, and used for filtering. Several filtering steps, based on variant frequency and location, were done to prioritize possible damaging variants (Described in Supplementary Table 2). Several modes of inheritance were considered, including *de novo*, compound heterozygous, recessive, and X-linked. Due to the low performance of the mother's sample in family 2 (Supplementary Table 1), this family was also analyzed without that sample, considering all rare variants possibly fitting the models above. Copy number variants (CNVs) were also assessed using an in-house read-depth based tool, comparing each subject to their parents (Aldrich et al. 2016; Halperin et al. 2017). Common variants in the Database of Genomic Variants (DGV) and technical artifacts were removed (MacDonald et al. 2014). Relationships (paternity and maternity) were confirmed by checking the inheritance of rare variants from each parent and the percentage of shared heterozygous variants between subject (child) and mother or father in each trio.

Sanger sequencing was performed by Polymerase Chain Reaction (PCR) followed by direct sequencing of the PCR product by both Forward and Reverse primers, performed on an ABI3130XL sequencer (Applied Biosystems Inc., Foster City, USA).

Greb1l RNA expression profiling during craniofacial and inner ear development

To study the expression of Greb1l in the developing and adult inner ear, both in-house and previously generated datasets by other researchers were analyzed *in silico*.

First, to evaluate the expression of Greb1l during mouse craniofacial development, processed expression values were downloaded from study GSE55967 from the Gene Expression Omnibus (GEO) database (National Institutes of Health) (Brunskill et al. 2014). This dataset was created by Brunskill et al. and contains craniofacial gene expression data from mouse embryos at stages E8.5, E9.5, and E10.5 (CD1 outbred mice) (Brunskill et al. 2014). RNA analysis was done via the Affymetrix Mouse Gene 1.0 ST Array (GPL6246) and RNA-seq (Nugen RiboSpia Ovation Pico WTA System V2). Processed data, as described in (Brunskill et al. 2014), containing the Fragments Per Kilobase of transcript per Million mapped reads (FPKM) values for RNA-seq and normalized expression values for micro-array data were downloaded and further analyzed with R3.1.2. For comparisons between different sample preparations and time points, we converted FPKM values to TPM (Transcripts Per Kilobase Million). We plotted all data using ggplot2.

To study the expression of Greb1l during mouse inner ear development and the adult inner ear, processed expression data were downloaded from the Shared Harvard Inner Ear Laboratory Database (SHIELD) database (Shen et al. 2015). First, a dataset containing RNA micro-array expression data of spiral and vestibular ganglion neurons collected at six developmental stages by Lu et al. was studied. This dataset was generated using the Affymetrix Mouse 430 v.2 GeneChips (Lu et al. 2011). Second, an RNA-seq dataset containing cochlea and utricles expression data from mice expressing EGFP under the Pou4f3 promoter (a hair cell marker) was downloaded. Scheffer et al. collected hair cells (GFP+) and surrounding cells (GFP-) separately using FACS for RNA extraction (Scheffer et al. 2015). Third, micro-array data (GeneChip Mouse Gene 2.0 ST) from adult mouse inner hair cells (IHCs) and outer hair cells (OHCs) created by Liu et al. were downloaded (Liu et al. 2014). Data on Greb1l and other genes of interest were extracted, further processed and plotted using ggplot2 in R.

Lastly, to study expression in the human ear, an in-house dataset of human tissue expression, including inner ear tissue, was analyzed (Schrauwen et al. 2016). This dataset contains RNA-sequencing data from the cochlea, ampulla, saccule, and utricle of the adult human inner ear derived from fresh surgically resected tissue from four adult donors with normal hearing. In addition, the transcriptome of 32 other human tissues was analyzed. Sequencing was done using a HiSeq 2000 instrument, and data were analyzed as mentioned before (Schrauwen et al. 2016). Normalized counts were plotted as the regularized logarithm (rLog). Custom scripts in R or ggplot2 were used to visualize output.

Immunohistochemistry

Formalin-fixed paraffin-embedded (FFPE) inner ear tissues from p0 or p7 Swiss mice previously prepared for other studies were used (Cryns et al. 2003). 8μm sections were mounted on positively charged slides. Immunohistochemistry was done using a Leica BondMax (Leica Biosystems, Wetzlar, Germany) following the Biocare Bond polymer RAB protocol (Biocare Medical, Pacheco, CA). In short, slides were first washed in triplicate with the Bond dewax solution at 72C, followed by 3 washes in ethanol. Next, a heat-induced antigen retrieval step was done in citrate buffer (Ph 6.0; 100 C) for 10 minutes. Then, slides were blocked in protein block and Rodent block M solution for 15 min each, followed by a 20-minute Avidin & Biotin block. Slides were incubated in Rabbit primary antibodies targeting greb1L (1/50-1/100 dilutions nbp2-32595 and hpa044218), for 30 minutes followed by a Rabbit Biocare Probe and polymer for 10 min each at room temperature. After this, slides were blocked in peroxide block for 5 minutes followed by mixed DAB refine and enhancer solution for 10 minutes and 1 minute respectively. Last, slides were stained with a Hematoxylin counterstain. All steps were separated by triplicate wash steps in Bond wash solution. Negative controls without primary antibody were run in parallel with the positive slides and showed no brown staining. Pictures were taken at 20x with the Leica ScanScope Aperio microscope (Leica Biosystems, Wetzlar, Germany).

Zebrafish *(Danio Rerio)* animals

Greb1l$^{-/-}$ fish carrying the *greb1l*^{sa16374} variant [c.1492C>T: p.(Gln408Ter)] were obtained from Zebrafish International Resource Center. Embryos were produced by paired matings of heterozygous zebrafish raised on a 14:10 hour light-dark cycle at 28.5°C. Genotyping was performed using GoTaq DNA polymerase (Promega, Madison, WI) following the tetra-primer ARMS-PCR method (Ye et al. 2001).

Zebrafish immunohistochemistry

Embryos were anesthetized with tricaine in embryo medium (Westerfield 1993), and fixed at 72 hours post fertilization (hpf) in 4% paraformaldehyde in phosphate-buffered saline (PBS; pH 7.2) overnight at 4°C. They were then rinsed once and washed 3 × 5 minutes in PBSX (PBS + O.5% Triton X-100), 3 × 1 hour in distilled H_2O, and blocked for one hour at room temperature in blocking solution (0.5% goat serum, 1% dimethylsulfoxide [DMSO], 0.2% Triton X-100, 2mg/ml bovine serum albumin [BSA], 1X PBS). Embryos were then incubated overnight at room temperature in monoclonal anti-tubulin, acetylated antibody (mouse, 1:1000, Sigma T6793) rinsed once and washed 3 × 1 hour at room temperature in PBSX. Finally, the embryos were incubated overnight in Alexa Fluor 488 goat anti-mouse (1:1000, Thermo Fisher) and Hoechst 33342 (1:1000, Thermo Fisher), and rinsed once and washed 3 × 30 minutes in PBSX. All fluorescently stained samples were mounted in low melting point agarose and imaged on a Zeiss LSM800 confocal microscope. After imaging, genomic DNA was extracted and animals were genotyped by PCR. Image stacks were coded to hide genotype and then analyzed by an independent observer. Images in figures are represented as maximum intensity projections.

Results

Clinical evaluation

Affected subject 1 showed an absent cochlea on the right, incomplete partition type I, and narrow cochlear aperture on the left. The subject showed bilateral abnormal and enlarged vestibules, dysplastic SCCs, and narrow IACs bilaterally. We were unable to determine the contents of lateral IACs secondary to how narrow the IACs were, but one nerve was present in the cistern on the right (likely facial) and two nerves in the cistern on the left (Fig 1C; Age 1 year). The second subject had absent cochleae bilaterally with enlarged vestibules and dysplastic SCCs (Fig 1D–E; Age 2–9 months). He also had two nerves in the right lateral IAC and one nerve in the left lateral IAC. Both individuals, to date, have a normal middle and outer ear, and have not developed other medical or developmental problems other than speech and hearing. The first affected subject underwent a cochlear implant on the left side with no measurable benefit or sound awareness postoperatively. The second affected subject did not undergo CI as he had no cochleae. Both individuals underwent placement of a right-sided auditory brainstem implant (ABI) and intraoperatively were confirmed to have absent 8^{th} nerves. Facial nerves were present and normal in both affected subjects. Facial nerve function and the remainder of the cranial nerve examinations were normal as well.

In addition to an extensive hearing evaluation, several additional tests were done to exclude other possible abnormalities in these subjects. A brain magnetic resonance imaging (MRI) and physical exam was performed in both individuals to exclude any other central nervous system abnormalities. The individuals in this study exhibited no hearing on either side measured via ABR and behavioral testing. Neither of these individuals were identified as having renal anomalies on urinalysis, and were otherwise healthy. A renal ultrasound was also performed in affected subject 1, and was normal.

Exome sequencing identifies *de novo* loss-of-function variants in *GREB1L*

Exome sequencing lead to the identification of a shared genetic etiology in both affected subjects. After filtering and prioritization of possibly damaging variants, only rare variants in the *GREB1L* gene were found to be shared between both families (Supplementary Tables 2 & 3). In the first trio, we identified a *de novo* splice site variant in *GREB1L* in the affected subject (ENST00000424526.5:c.4368G>T) (Figs 1A and S3). This variant is predicted to be a loss of the 5′ donor site at that position by multiple splice bioinformatics tools including dbscSNV1.1 (ADA and RF score of 0.999993 and 1.0 respectively) (Jian et al. 2014). A loss of function at this 5′ donor site is expected to lead to exon skipping and a premature frameshift [ENSP00000412060.1:p.(Glu1410AspfsTer3) or p.(Glu1410fs)]. The aberrant mRNA is predicted to be targeted by nonsense-mediated decay (Maquat 2004). This variant has a Combined Annotation Dependent Depletion (CADD) score of 26.1 (Kircher et al. 2014).

Exome sequencing of the second affected subject and parents identified a *de novo* nonsense variant in *GREB1L* in the subject [ENST00000424526.5:c.982C>T; ENSP00000412060.1:p.(Arg328Ter)] (Figs 1B and S4), which is predicted to be targeted by

nonsense-mediated decay (Maquat 2004). This variant has a CADD score of 21.6 (Kircher et al. 2014).

Both variants were confirmed with Sanger sequencing, and are not present in the gnomAD browser of 126,216 exome sequenced and 15,136 whole-genome sequenced individuals (Lek et al. 2016). Both variants are likely a loss-of-function (LOF). Both variants have been deposited in ClinVar (Accession numbers #SCV000611707 and #SCV000611708). Additional variants of unknown significance can be found in Supplementary Table S3. No rare CNVs were identified.

Greb1l expression during early mouse craniofacial development

By analyzing Greb1l expression in a dataset created by Brunskill et al. (Brunskill et al. 2014), we show that the expression of Greb1l peaks at E8.5 during the early craniofacial development in mice, and decreases in expression during E9.5 and E10.5. In addition, Greb1l expression is wide-spread and non-compartmentalized (Figs 2A and B). Greb1l shows a preferred expression in the craniofacial mesoderm, the caudal brain neural epithelium and flanking neuroepithelium, including floorplate and more dorsal non-floor plate. Expression in the otic vesicle at E9.5 is intermediate.

Greb1l expression in the developing and adult inner ear

By re-analyzing inner ear expression data of an in-house dataset and data generated by several other researchers (Lu et al. 2011; Liu et al. 2014; Scheffer et al. 2015; Schrauwen et al. 2016), we demonstrate that during the development of the mouse inner ear expression of Greb1l is highly prominent in the spiral ganglion, vestibular ganglion, and peaks at E13–E16, after which it decreases, but still remains present (Fig 2C). In the cochlea and utricle inner hair cells or surrounding cells, a similar peak is seen at E16, after which expression decreases (Fig 2D). In the adult mouse cochlea, RNA expression can be measured in the outer and inner hair cells (Fig S5). Expression in adult human tissues is widespread, and expression in the cochlea is prominent (Fig S6).

Immunohistochemistry at P0 and P7 showed a widespread expression in the mouse inner ear, with a high presence in the spiral ganglia, cochlear nerve bundles, hair cells, supporting cells, and more (Figs S7 and S8).

Greb1l$^{-/-}$ zebrafish show sensory epithelia innervation abnormalities

The *Greb1l*$^{-/-}$ zebrafish studied here (sa16374; zfin.org) contains a c.1492C>T variant (ENSDART00000057268) resulting in a premature stop codon p.(Gln408Ter). Heterozygous *greb1l* zebrafish were mated to obtain offspring (F1) with a theoretical distribution of 25% of wild-type, 50% heterozygotes, and 25% of *greb1l* mutant homozygotes. The embryos were fixed, stained, and imaged at 72hpf as described to identify innervation abnormalities within the inner ear associated with the homozygous *greb1l* variant. Of the 92 embryos analyzed, 22 (24%) were homozygous for the *greb1l* variant. The mutant embryos exhibited a loss of the anterior cristae nerve (17/22 mutants, 77.3%), an abnormal innervation pathway from the occipital lateral line neuromast (2/22, 9.1%), or both abnormalities (3/22, 13.6%) (Fig 3). No abnormalities were observed in wild-type or heterozygous animals. The hearing

function of *greb1l* mutants was evaluated using the startle response behavior test at 5 and 14 dpf (Yang et al. 2017). No functional hearing or vestibular deficits were observed.

Discussion

Abnormalities in cochleovestibular anatomy can provide greater than normal challenges for cochlear implant surgery and programming, leading to variable results (Chadha et al. 2009; Kaga 2017). Deaf newborn children that have abnormal inner ear anatomy and/or an abnormal CVN could potentially be considered for an auditory brainstem implant (ABI) instead of a cochlear implantation (CI) (Colletti et al. 2013). However, current clinical imaging protocols are not fully able to consistently provide cochlear or auditory nerve status information to guide a surgeons' choice of an auditory prosthesis (Kari et al. 2018). Children with unfavorable anatomy for CI may be candidates for an ABI (Colletti et al. 2013), although this is currently not yet FDA-approved in the US in children under the age of 12. An ABI delivers the stimulation directly to the cochlear nuclei in the brainstem whereas a CI delivers the signal to the cochlear nerve fibers inside the cochlea. These two interventions carry significantly different risk profiles, and appropriate device selection is of utmost importance. The variability of language and hearing outcomes in children with abnormal CVNs receiving CIs/ABIs coupled with the current inability to predict their outcomes (Kari et al. 2018; Young et al. 2012; Colletti et al. 2013; Birman et al. 2016), leads to children enduring multiple assessments and interventions. The sensitive and critical time periods for auditory development are often exceeded by the time needed to determine the most suitable treatment or hindered due to efforts in attempting to understand the progression, delaying language acquisition. A molecular diagnosis is of great importance for potential patient management and family counseling. If it were possible to predict whether a child with a malformation has a benefit from a hearing aid or a cochlear implant, children could be spared several fruitless interventions. In addition, a molecular diagnosis might help us understand more about the underlying developmental defects, which could be able to guide us towards the correct intervention more rapidly, in a more 'personalized' setting.

In this study, we used exome sequencing to identify the underlying genetic defect in two unrelated affected subjects with rare and severe inner ear malformations. We identified *de novo* loss-of-function (LOF) variants in *GREB1L* in each affected subject [c.4368G>T; p.(Glu1410fs) and c.982C>T;p.(Arg328*)], suggesting that haploinsufficiency of GREB1L is the primary cause of disease.

Not much is known about the function of *GREB1L*, or Growth Regulation By Estrogen In Breast Cancer 1 Like. An important paralog of this gene is GREB1. GREB proteins might play a role in mediating cell growth (Rae et al. 2005). GREB1L has previously been identified as a premigratory neural crest (NC) regulatory molecule in *Xenopus laevis*. *Greb1L* was found enriched at the neural border in early neurulae, and maintained in the dorsal neural tube and NC (Plouhinec et al. 2014). CVN development involves cell populations from two disparate progenitors of the otic placode (neurons) and NC cells (glia) (Sandell et al. 2014; Pai 2017). The development of the ear is complex, with three distinctly different origins. Specifically, the inner ear derives from neuroectoderm, the middle ear comes from branchial arch mesoderm and endoderm, and the external ear arises from

branchial ectoderm. An exception are the melanocyte cells of the *stria vascularis* – the secretory epithelium of the cochlea – which are of NC origin (Torres and Giráldez 1998).

Defects of the strial melanocytes, associated with general neural crest defects, have been described in several mice and human mutants. Underlying genes code for a variety of molecules expressed in neural crest derivatives. However, the phenotypes of these mouse mutants are different from the phenotype of the affected subjects enrolled in this study (Torres and Giráldez 1998), and our data suggest that GREB1L might also be important in inner ear development and patterning.

To support this, we evaluated Greb1l RNA expression during craniofacial/inner ear development and the adult inner ear by further analyzing data generated by other researchers and in-house data (Figs 2, S5, S6). We found that Greb1l expression is widespread, and not highly compartmentalized during craniofacial development, and peaks at E8.5 and E13–E16, after which it declines during adulthood (Fig 2). In mice, the inner ear rises from a thickening of the ectoderm known as the otic placode at E7.5, and at E8.5 the otic placode invaginates to form the otocyst (Chi et al. 2009). At E9.5, the otocyst has closed and from here on to E14.5, complex and rapid morphological changes occur. During this time-frame the mature inner ear structure is formed, which is comprised of the semicircular canals, vestibule, and cochleae. At E12.5, all primordial structures have undergone further refinements, approximating their mature shape, and at E14.5, the membranous labyrinth has attained its mature shape, and the cochlea has reached one and a half turns (Chi et al. 2009). We show that Greb1l peaks in the very early development of the inner ear (E8.5 otic placode invagination), later in the maturing and the refinement of the formed cochlear, and vestibular shapes (E13–E16), supporting a possibly important role in early ear development.

This significant role of GREB1L in ear development is also supported by the phenotype of our affected subjects. In human development, during the third week, the otic placode appears on each side in the surface ectoderm. This becomes invaginated and forms the otic pit. At the end of the forth week, this is completely surrounded and forms the otic vesicle or otocyst (Sennaroglu and Saatci 2002). Sennaroglu suggested an inner ear malformation classification based on these various stages of embryogenesis of the inner ear. He suggested that an inner ear development arrest during the 3rd week is associated with Michel aplasia and cochlear aplasia (late 3rd week), a common cavity (arrest in the 4th week), and an incomplete partition I (5th week) (Sennaroglu and Saatci 2002) (Figs S1 and S2). The second subject included in this study had absent cochleae or cochlear aplasia (Figs 1D–E), suggestive for a developmental arrest during the late third week or very early development (otic placode invagination). Interestingly, during this period Greb1l expression also spikes in several craniofacial tissues in the mouse (equivalent to E8.5) (Fig 2). The first affected subject showed cochlear aplasia on the right, and incomplete partition type I and narrow cochlear aperture on the left. This reflects a more developed left ear in comparison to the right ear and phenotypic heterogeneity within the same affected subject.

Greb1l is also important in the organogenesis of various tissues and craniofacial development. Greb1l$^{-/-}$ knockout mice (c.64_68delATAG; p.Iso22Lysfs*39) are embryonically lethal and show a variety of organogenesis defects, including gonad

malformations, severe kidney and uterus defects, cardiac morphogenesis defects, but also severe craniofacial malformations, including exencephaly (De Tomasi et al. 2017). All the other organs (lung, liver, intestine, stomach) appear to be normal and well positioned, although slightly underdeveloped (De Tomasi et al. 2017). Severe craniofacial abnormalities were also observed in several F0 mutant mouse embryos for several mutations generated using CRISPR/Cas9 and harboring mosaicism (Brophy et al. 2017). Exencephaly and craniofacial dysmorphology including unilateral and bilateral cleft lip were observed. Greb1l shows a widespread expression in craniofacial tissues during development (Fig 2).

In addition to inner ear malformation, both our affected subjects also show defects of the 8th cranial nerve or CVN. To understand whether this might be due to a direct role in the development of the CVN, we studied a Greb1l$^{-/-}$ zebrafish (*Danio rerio*) (Fig 3). Zebrafish have patches of sensory epithelia in their inner ears (maculae and cristae), but also have sensory patches as part of their lateral line system, called neuromasts (Raible and Kruse 2000). Homozygous mutant embryos carrying a premature stop mutation (p.Gln408Ter) at 72hpf exhibited a loss of the anterior cristae nerve (77.3%), an abnormal innervation pathway from the occipital lateral line neuromast (9.1%), or both abnormalities (13.6%). This suggests that Greb1l is also important in the innervation of sensory epithelia and 8th cranial nerve development in addition to inner ear patterning and development. Note that in one of the two affected subjects, the IAC canal, which develops from the mesoderm (Yates et al. 1997), is also very narrow which might have hindered 8th cranial nerve development as well.

GREB1L has not previously been associated with human disease and hearing loss except, recently, three different studies independently showed that rare heterozygous variants in *GREB1L* are associated with congenital kidney malformations and agenesis in humans (Brophy et al. 2017; De Tomasi et al. 2017; Sanna-Cherchi et al. 2017), zebrafish, and mice (Brophy et al. 2017; De Tomasi et al. 2017). This is a fairly common disease (i.e. 0.5% of the general population), and variants in *GREB1L* account for a small fraction (3.5%) of these cases (Sanna-Cherchi et al. 2017). Haploinsufficiency has been suggested as the mechanism leading to the phenotype due to the high number of LOF variants found. We suspect this to be the leading mechanism in our affected subjects with inner ear malformations as well. Haploinsufficiency of *GREB1L* in humans is further supported by the extreme rarity of LOF variants in *GREB1L* in control populations such as ExAC, DECIPHER and Bravo (TOPMed) (Firth et al. 2009; Lek et al. 2016). In addition, haploinsufficiency predictions for this gene indicate it is likely to exhibit haploinsufficiency (Haploinsufficiency Score of 9.33%) (Huang et al. 2010).

We previously identified compound heterozygous variants in *MASP1* in a child with absent cochlear nerves and vestibular anomalies (Kari et al. 2017). Mutations in *MASP1* cause 3MC syndrome or craniofacial-ulnar-renal syndrome (Rooryck et al. 2011), which has a large phenotypic variability, including a spectrum of features such as developmental delay, intellectual disability, facial features, hearing loss, short stature, skeletal abnormalities and kidney abnormalities (Kari et al. 2017). MASP1 is involved in the development of the ear, kidneys and several other tissues during the embryonic period. A study shows it is involved in the early guidance of the migration of neural crest (NC) cells during embryonic

development (Rooryck et al. 2011), which is noteworthy as *GREB1L* was identified as a premigratory NC regulatory molecule as well (Plouhinec et al. 2014).

Furthermore, it is interesting that *de novo*/dominant mutations in *GREB1L* can cause pleiotropic phenotypes in humans. As suggested by the mouse model, greb1l is involved in early development of multiple tissues (De Tomasi et al. 2017), and can manifest as pleiotropic disorders in humans. What is seen here for *GREB1L* could be comparable to *EYA1*. Phenotypic variation in patients with *EYA1* variants causing Branchio-oto-renal (BOR)/branchio-otic (BO) syndrome is high, even within the same family (Orten et al. 2008). The severity of the phenotype does not correlate with type of variant nor with the domain involved. We do not see a particular genotype-phenotype relation in *GREB1L* variants as well (Brophy et al. 2017; Boissel et al. 2017; De Tomasi et al. 2017; Sanna-Cherchi et al. 2017), and LOF is a suspected mechanism for kidney malformations as well. In BOR patients with *EYA1* mutations, normal kidneys were often seen in other affected members of the same families (Orten et al. 2008). Similar to *MASP1* and *GREB1L*, *EYA1* is also important in the regulation of neural crest cells and morphogenesis of several organs (Xu et al. 2002). This suggests that environmental factors or other genetic modifiers during embryogenesis and development of the child contribute to the phenotypic variance in *GREB1L* and *EYA1.* Environmental factors, particularly nutrition of the mother during pregnancy, have been shown to affect the fetus development and development of disorders (Marques et al. 2013). In addition, children born with mild malformations can show a significant increase in severity due to infections, nutrition, drug treatment, or other environmental factors (Orten et al. 2008). Last, as hearing was not assessed in the patients with *GREB1L* renal disease, mild hearing/vestibular defects might be present.

In conclusion, we suggest that GREB1L is crucial in the early development of the inner ear and the development of sensory epithelia innervation. This is supported by: 1) The identification of two novel *de novo* variants in unrelated subjects with similar and unique inner ear and 8th cranial nerve anomalies; 2) The variants result in a LOF in a gene that is likely to exhibit haploinsufficiency; 3) GREB1L has been identified as a premigratory neural crest (NC) regulatory molecule and is involved in the embryonic development of many tissues. This is similar to *MASP1*, which we previously identified in a child with distinct inner ear and cochlear nerve anomalies; 4) Greb1l shows various spikes in expression during developing craniofacial tissues and decreases during adulthood; 5) We show a disruption of sensory epithelia innervation in *Greb1l*$^{-/-}$ zebrafish. Last, a genetic diagnosis and understanding of the molecular basis might help with identifying the correct therapeutic intervention for affected subjects with unique inner ear abnormalities and hearing problems.

Supplementary Material

Refer to Web version on PubMed Central for supplementary material.

Acknowledgments

The authors thank the families for participating in this study. This study was supported by private donations to TGen's Center for Rare Childhood Disorders (https://www.tgen.org/giving/tgen-foundation/), the American Hearing Research Foundation to I.S. (http://american-hearing.org/), R01 010856 (https://www.nih.gov/) and the

Mills Auditory Foundation (http://millsauditoryfoundation.org/) to R.A.F. We would like to acknowledge Brunskill et al, Lu et al, Liu et al, and Scheffer et al, for the creation and public deposition of their RNA expression data that was used in this study.

References

Aldrich J, Keats JJ, Liang WS, et al. Abstract 45: Detection of focal somatic copy number variants in whole genome, whole exome, and targeted next-generation sequencing data of tumor/normal pairs. Clin Cancer Res. 2016; 22:45–45. DOI: 10.1158/1557-3265.PMSCLINGEN15-45

Birman CS, Powell HRF, Gibson WPR, Elliott EJ. Cochlear Implant Outcomes in Cochlea Nerve Aplasia and Hypoplasia. Otol Neurotol. 2016; 37:438–445. DOI: 10.1097/MAO.0000000000000997 [PubMed: 27050647]

Boissel S, Fallet-Bianco C, Chitayat D, et al. 2017; Genomic study of severe fetal anomalies and discovery of GREB1L mutations in renal agenesis. Genet Med. doi: 10.1038/gim.2017.173

Brophy PD, Rasmussen M, Parida M, et al. A Gene Implicated in Activation of Retinoic Acid Receptor Targets is a Novel Renal Agenesis Gene in Humans. Genetics genetics. 2017; 1125.2017. doi: 10.1534/genetics.117.1125

Brunskill EW, Potter AS, Distasio A, et al. A gene expression atlas of early craniofacial development. Dev Biol. 2014; 391:133–46. DOI: 10.1016/j.ydbio.2014.04.016 [PubMed: 24780627]

Chadha NK, James AL, Gordon KA, et al. Bilateral Cochlear Implantation in Children With Anomalous Cochleovestibular Anatomy. Arch Otolaryngol Neck Surg. 2009; 135:903.doi: 10.1001/archoto.2009.120

Chi F-L, Han Z, Dai P-D, et al. Three-dimensional reconstruction of C57BL/6 mouse inner ear during development. ORL J Otorhinolaryngol Relat Spec. 2009; 71:334–41. DOI: 10.1159/000272029 [PubMed: 20068376]

Cingolani P, Platts A, Wang LL, et al. A program for annotating and predicting the effects of single nucleotide polymorphisms, SnpEff: SNPs in the genome of Drosophila melanogaster strain w1118; iso-2; iso-3. Fly (Austin). 2012; 6:80–92. DOI: 10.4161/fly.19695 [PubMed: 22728672]

Colletti L, Wilkinson EP, Colletti V. Auditory brainstem implantation after unsuccessful cochlear implantation of children with clincal diagnosis of cochlear nerve deficiency. Ann Otol Rhinol Laryngol. 2013; 122:605–612. [PubMed: 24294682]

Cryns K, Thys S, Van Laer L, et al. The WFS1 gene, responsible for low frequency sensorineural hearing loss and Wolfram syndrome, is expressed in a variety of inner ear cells. Histochem Cell Biol. 2003; 119:247–56. DOI: 10.1007/s00418-003-0495-6 [PubMed: 12649740]

De Tomasi L, David P, Humbert C, et al. Mutations in GREB1L Cause Bilateral Kidney Agenesis in Humans and Mice. Am J Hum Genet. 2017; 101:803–814. DOI: 10.1016/j.ajhg.2017.09.026 [PubMed: 29100091]

Firth HV, Richards SM, Bevan AP, et al. DECIPHER: Database of Chromosomal Imbalance and Phenotype in Humans Using Ensembl Resources. Am J Hum Genet. 2009; 84:524–533. DOI: 10.1016/j.ajhg.2009.03.010 [PubMed: 19344873]

Halperin RF, Carpten JD, Manojlovic Z, et al. A method to reduce ancestry related germline false positives in tumor only somatic variant calling. BMC Med Genomics. 2017; 10:61.doi: 10.1186/s12920-017-0296-8 [PubMed: 29052513]

Huang N, Lee I, Marcotte EM, Hurles ME. Characterising and Predicting Haploinsufficiency in the Human Genome. PLoS Genet. 2010; 6:e1001154.doi: 10.1371/journal.pgen.1001154 [PubMed: 20976243]

Jackler RK, Luxford WM, House WF. Congenital malformations of the inner ear: A classification based on embryogenesis. Laryngoscope. 1987; 97:2–14. [PubMed: 3821363]

Jian X, Boerwinkle E, Liu X. In silico prediction of splice-altering single nucleotide variants in the human genome. Nucleic Acids Res. 2014; 42:13534–13544. DOI: 10.1093/nar/gku1206 [PubMed: 25416802]

Kaga K. Cochlear Implantation in Children with Inner Ear Malformation and Cochlear Nerve Deficiency. Springer Singapore; Singapore: 2017. Overview; 1–9.

Kaplan AB, Kozin ED, Puram SV, et al. Auditory brainstem implant candidacy in the United States in children 0–17 years old. Int J Pediatr Otorhinolaryngol. 2015; 79:310–315. DOI: 10.1016/j.ijporl.2014.11.023 [PubMed: 25577282]

Kari E, Go JL, Loggins J, et al. Abnormal cochleovestibular nerves and pediatric hearing outcomes: patients with “absent cochlear nerves” can derive benefit from cochlear implantation. Otol Neurotol. 2018 In Press.

Kari E, Schrauwen I, Llaci L, et al. Compound heterozygous mutations in *MASP1* in a deaf child with absent cochlear nerves. Neurol Genet. 2017; 3:e153.doi: 10.1212/NXG.0000000000000153 [PubMed: 28534045]

Kircher M, Witten DM, Jain P, et al. A general framework for estimating the relative pathogenicity of human genetic variants. Nat Genet. 2014; 46:310–5. DOI: 10.1038/ng.2892 [PubMed: 24487276]

Langmead B, Trapnell C, Pop M, Salzberg SL. Ultrafast and memory-efficient alignment of short DNA sequences to the human genome. Genome Biol. 2009; 10:R25.doi: 10.1186/gb-2009-10-3-r25 [PubMed: 19261174]

Lek M, Karczewski KJ, Minikel EV, et al. Analysis of protein-coding genetic variation in 60,706 humans. Nature. 2016; 536:285–91. DOI: 10.1038/nature19057 [PubMed: 27535533]

Liu H, Pecka JL, Zhang Q, et al. Characterization of Transcriptomes of Cochlear Inner and Outer Hair Cells. J Neurosci. 2014; 34:11085–11095. DOI: 10.1523/JNEUROSCI.1690-14.2014 [PubMed: 25122905]

Liu X, Wu C, Li C, Boerwinkle E. dbNSFP v3.0: A One-Stop Database of Functional Predictions and Annotations for Human Nonsynonymous and Splice-Site SNVs. Hum Mutat. 2016; 37:235–241. DOI: 10.1002/humu.22932 [PubMed: 26555599]

Lu CC, Appler JM, Houseman EA, Goodrich LV. Developmental profiling of spiral ganglion neurons reveals insights into auditory circuit assembly. J Neurosci. 2011; 31:10903–18. DOI: 10.1523/JNEUROSCI.2358-11.2011 [PubMed: 21795542]

MacDonald JR, Ziman R, Yuen RKC, et al. The Database of Genomic Variants: a curated collection of structural variation in the human genome. Nucleic Acids Res. 2014; 42:D986–92. DOI: 10.1093/nar/gkt958 [PubMed: 24174537]

Maquat LE. Nonsense-mediated mRNA decay: splicing, translation and mRNP dynamics. Nat Rev Mol Cell Biol. 2004; 5:89–99. DOI: 10.1038/nrm1310 [PubMed: 15040442]

Marques AH, O’Connor TG, Roth C, et al. The influence of maternal prenatal and early childhood nutrition and maternal prenatal stress on offspring immune system development and neurodevelopmental disorders. Front Neurosci. 2013; 7:120.doi: 10.3389/fnins.2013.00120 [PubMed: 23914151]

Masuda S, Usui S, Matsunaga T. High prevalence of inner-ear and/or internal auditory canal malformations in children with unilateral sensorineural hearing loss. Int J Pediatr Otorhinolaryngol. 2013; 77:228–232. DOI: 10.1016/j.ijporl.2012.11.001 [PubMed: 23200870]

McKenna A, Hanna M, Banks E, et al. The Genome Analysis Toolkit: a MapReduce framework for analyzing next-generation DNA sequencing data. Genome Res. 2010; 20:1297–303. DOI: 10.1101/gr.107524.110 [PubMed: 20644199]

Orten DJ, Fischer SM, Sorensen JL, et al. Branchio-oto-renal syndrome (BOR): novel mutations in the *EYA1* gene, and a review of the mutational genetics of BOR. Hum Mutat. 2008; 29:537–544. DOI: 10.1002/humu.20691 [PubMed: 18220287]

Pai I. Cochlear Implantation in Children with Inner Ear Malformation and Cochlear Nerve Deficiency. Springer Singapore; Singapore: 2017. Embryology of Cochlear Nerve and Its Deficiency; 19–27.

Plouhinec J-L, Roche DD, Pegoraro C, et al. Pax3 and Zic1 trigger the early neural crest gene regulatory network by the direct activation of multiple key neural crest specifiers. Dev Biol. 2014; 386:461–472. DOI: 10.1016/j.ydbio.2013.12.010 [PubMed: 24360906]

Pryor SP. SLC26A4/PDS genotype-phenotype correlation in hearing loss with enlargement of the vestibular aqueduct (EVA): evidence that Pendred syndrome and non-syndromic EVA are distinct clinical and genetic entities. J Med Genet. 2005; 42:159–165. DOI: 10.1136/jmg.2004.024208 [PubMed: 15689455]

Rae JM, Johnson MD, Scheys JO, et al. GREB1 is a critical regulator of hormone dependent breast cancer growth. Breast Cancer Res Treat. 2005; 92:141–149. DOI: 10.1007/s10549-005-1483-4 [PubMed: 15986123]

Raible DW, Kruse GJ. Organization of the lateral line system in embryonic zebrafish. J Comp Neurol. 2000; 421:189–98. [PubMed: 10813781]

Rooryck C, Diaz-Font A, Osborn DPS, et al. Mutations in lectin complement pathway genes COLEC11 and MASP1 cause 3MC syndrome. Nat Genet. 2011; 43:197–203. DOI: 10.1038/ng.757 [PubMed: 21258343]

Sandell LL, Butler Tjaden NE, Barlow AJ, Trainor PA. Cochleovestibular nerve development is integrated with migratory neural crest cells. Dev Biol. 2014; 385:200–210. DOI: 10.1016/j.ydbio.2013.11.009 [PubMed: 24252775]

Sanna-Cherchi S, Khan K, Westland R, et al. Exome-wide Association Study Identifies GREB1L Mutations in Congenital Kidney Malformations. Am J Hum Genet. 2017; 101:789–802. DOI: 10.1016/j.ajhg.2017.09.018 [PubMed: 29100090]

Scheffer DI, Shen J, Corey DP, Chen Z-Y. Gene Expression by Mouse Inner Ear Hair Cells during Development. J Neurosci. 2015; 35:6366–80. DOI: 10.1523/JNEUROSCI.5126-14.2015 [PubMed: 25904789]

Schrauwen I, Hasin-Brumshtein Y, Corneveaux JJ, et al. A comprehensive catalogue of the coding and non-coding transcripts of the human inner ear. Hear Res. 2015; doi: 10.1016/j.heares.2015.08.013

Sennaroglu L, Bajin MD. Cochlear Implantation in Children with Inner Ear Malformation and Cochlear Nerve Deficiency. Springer Singapore; Singapore: 2017. Classification of Inner Ear Malformations; 61–85.

Sennaroglu L, Saatci I. A new classification for cochleovestibular malformations. Laryngoscope. 2002; 112:2230–2241. DOI: 10.1097/00005537-200212000-00019 [PubMed: 12461346]

Shen J, Scheffer DI, Kwan KY, Corey DP. SHIELD: an integrative gene expression database for inner ear research. Database (Oxford). 2015; 2015:bav071. doi: 10.1093/database/bav071

Torres M, Giráldez F. The development of the vertebrate inner ear. Mech Dev. 1998; 71:5–21. DOI: 10.1016/S0925-4773(97)00155-X [PubMed: 9507049]

Westerfield M. The Zebrafish Book: A Guide for the Laboratory Use of Zebrafish (Brachydanio … - Monte Westerfield - Google Books. 2. University of Oregon Press; Eugene: 1993.

Xu P-X, Zheng W, Laclef C, et al. Eya1 is required for the morphogenesis of mammalian thymus, parathyroid and thyroid. Development. 2002; 129:3033–44. [PubMed: 12070080]

Yamamoto N, Kanno A, Matsunaga T. Cochlear Implantation in Children with Inner Ear Malformation and Cochlear Nerve Deficiency. Springer Singapore; Singapore: 2017. Genetics of Inner Ear Malformation and Cochlear Nerve Deficiency; 47–59.

Yang Q, Sun P, Chen S, et al. Behavioral methods for the functional assessment of hair cells in zebrafish. Front Med. 2017; 11:178–190. DOI: 10.1007/s11684-017-0507-x [PubMed: 28349300]

Yates JA, Patel PC, Millman B, Gibson WS. Isolated congenital internal auditory canal atresia with normal facial nerve function. Int J Pediatr Otorhinolaryngol. 1997; 41:1–8. [PubMed: 9279630]

Ye S, Dhillon S, Ke X, et al. An efficient procedure for genotyping single nucleotide polymorphisms. Nucleic Acids Res. 2001; 29:E88–8. [PubMed: 11522844]

Young NM, Kim FM, Ryan ME, et al. Pediatric cochlear implantation of children with eighth nerve deficiency. Int J Pediatr Otorhinolaryngol. 2012; 76:1442–1448. DOI: 10.1016/j.ijporl.2012.06.019 [PubMed: 22921779]

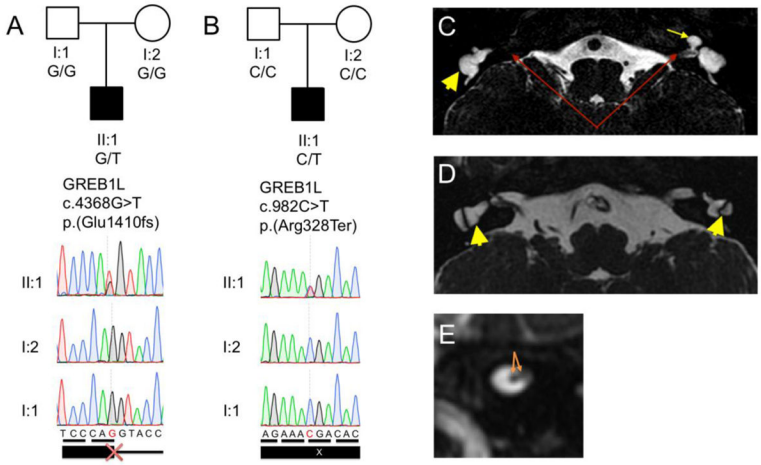

Fig. 1. Genetic and imaging data of the families enrolled in this study

A. Pedigree of family 1 with Sanger sequencing traces. **B.** Pedigree of family 2 with Sanger sequencing traces. Both affected subjects have a *de novo* loss-of-function mutation in the *GREB1L* gene. **C.** Affected subject one's MRI shows dysplastic SCCs, enlarged vestibules, absent cochlea on the right (yellow arrowhead), and incomplete partition type I (IP-I) on the left (yellow arrow). The diameters of his IACs were too narrow to determine the neural contents on imaging (red arrows). **D.** Affected subject two's MRI shows bilateral absent cochleae, enlarged vestibules, and dysplastic SCCs (yellow arrowheads). **E.** Oblique cross-sectional imaging of the IAC on MRI showed that he has two nerves in the right IAC (shown, orange arrows), and one on the left (not shown), normal = 4.

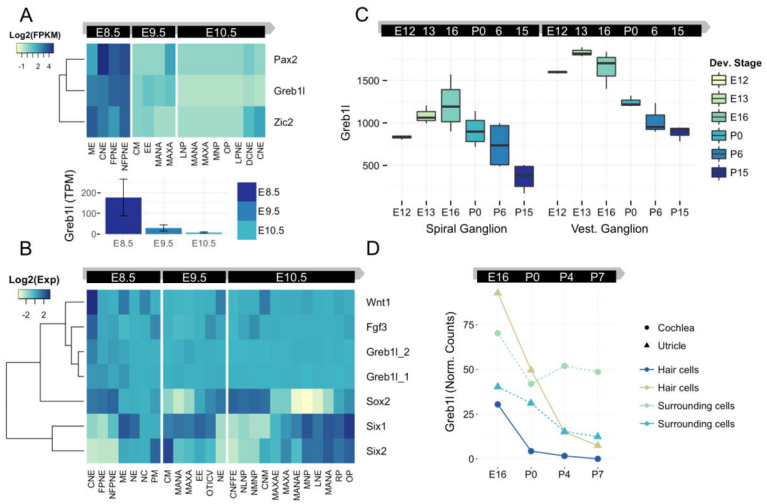

Fig. 2. Greb1l RNA expression in various craniofacial tissues and the inner ear during the development of the mouse

A/B. RNA expression data from various laser capture microdissected (LCM) tissues during early mouse craniofacial development (Brunskill et al. 2014).

A. RNA-Seq profiling shows that Greb1l is expressed with preference during E8.5 in early development. This expression decreases over E9.5 and E10.5. In the above panel, tissue expression is plotted together with *Pax2* and *Zic2* that show a similar expression profile, both important genes in mouse inner ear development. A higher expression is observed in the craniofacial mesoderm, the caudal brain neural epithelium, and flanking neuroepithelium, including floorplate and more dorsal non-floor plate compared to other craniofacial tissues. The lower panel shows the average Greb1l expression per developmental stage over all tissues in TPM values to illustrate decreased expression over time. Blue = high expression; Green=intermediate expression; Yellow=low expression.

B. Micro-array RNA expression analysis of mouse craniofacial tissues during early development demonstrates a widespread and non-compartmentalized expression of Greb1l. This in contrast to *Six1, 2* and *Sox2*, but similar to *Fgf3* and *Wnt1* (given as an example). The highest expression is also seen during E8.5, similar to the RNA-seq data in A. An intermediate expression in the otic vesicle is seen at E9.5. Blue = high expression; Green=intermediate expression; Yellow=low expression. Greb1l_1 and Greb1l_2 indicate the two different probes used for greb1l on the microarray respectively (10453797, 10453811). For A/B data were downloaded and further analyzed from study GSE55967 (Brunskill et al. 2014) from the Gene Expression Omnibus (GEO) database (National Institutes of Health).

C. Micro-array RNA expression data of Greb1l in Spiral and vestibular ganglion neurons collected at six developmental stages (Lu et al. 2011). This shows that Greb1l (probe set 1439341) is expressed in the inner ear ganglia during development and upregulated during E13-E16 after which it slowly decreases in expression.

D. RNA-Seq data from cochlea and utricles from mice expressing EGFP under the Pou4f3 promoter (hair cell marker). Hair cells (GFP+) and surrounding cells (GFP-) were separately collected using FACS for RNA extraction (Scheffer et al. 2015). Greb1l is expressed in both the hair cells and surrounding cells of the utricle and cochlea with the highest expression

during E16. The Y-axis represents the normalized read counts from the DEseq package. C/D Data were obtained from the Shared Harvard Inner Ear Laboratory Database (SHIELD) database (Lu et al. 2011; Shen et al. 2015; Scheffer et al. 2015), and further analyzed here. Craniofacial tissue codes: B. NE: Neuroepithilium; NC: Neural Crest; PM: Paraxial mesoderm; CNE (E8.5): caudal neural epithelium; FPNE: floor plate neural epithelium; ME: mesenchyme; NFPNE: non-floor plate neural epithelium; CM: Cranial Mesenchyme; EE: epidermal ectoderm; MANA: mandibular arch; MAXA: maxillary arch; OTICV: Otic vesicle; CNM: central neuroepithelium midline; CNFFE: control neuroepithelium not flanking facial emincences; LNE: lateral nasal eminence; MANAE: mandibular arch epidermal ectoderm; MAXAE: maxillary arch epidermal ectoderm; MNP: medial nasal prominence; NLNP: neuroepithelium underlying lateral nasal prominence; NMNP: neuroepithelium underlying medial nasal prominence; OP: olfactory pit; RP: rathke's pouch; LNP: lateral nasal prominence; CNE (E10.5): central neural epithelium; CDNE: dorsal control neural epithelium; LPNE: lateral prominence neural epithelium.

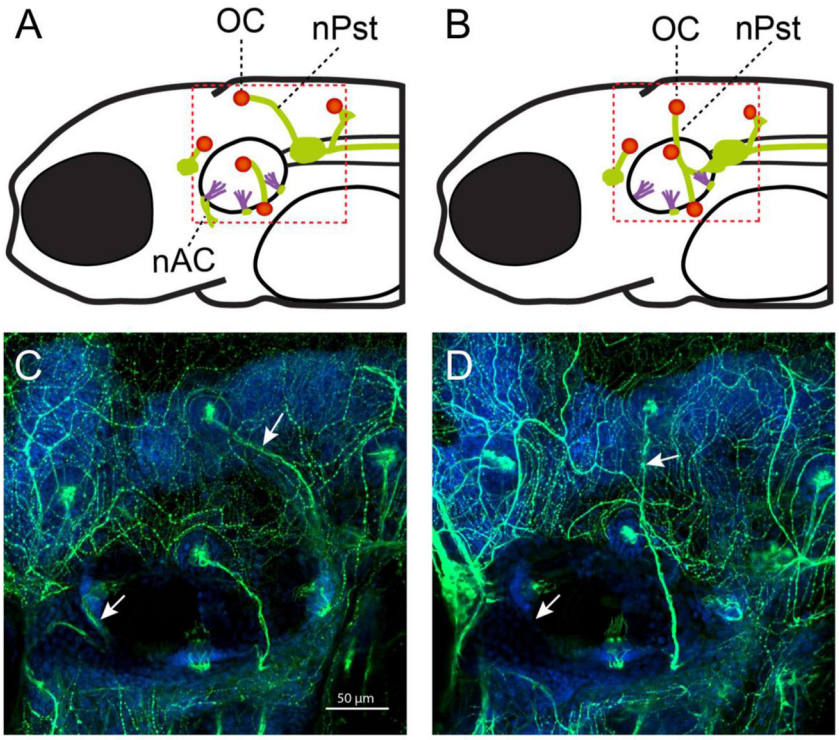

Fig 3. G*reb1l*$^{-/-}$ zebrafish show sensory epithelia innervation abnormalities

A. The stereotyped positions of lateral line neuromasts (red circles), the cristae of the inner ear (purple), and their nerves (green) in 72 hpf zebrafish (Raible and Kruse 2000). **B.** Loss of the anterior cristae nerve (nAC), and misrouting of the posterior nerve (nPst) of the occipital neuromast (OC) in a portion of *greb1l* mutant zebrafish. **C.** Wildtype zebrafish: arrows identifying normal nPst and nAC. **D.** Mutant *greb1l* zebrafish representing both abnormalities (absent nAC and abnormal nPst pathway). Blue: Hoechst, Green: Acetylated Tubulin.